

An Observational Analysis of an Especially Long-Lived Supercell in Montana

Matthew Ziebell
WFO Glasgow, Montana

Introduction

During the late morning of 16 June 2007, a supercell thunderstorm developed across far north central Montana. Over the next 10 hours this storm traveled approximately 483 km (300 miles), producing flash flooding, hail up to 7.62 cm (2.75 inches) in diameter, and wind gusts up to 143 km/hr (89 miles/hr) before terminating near the Montana-North Dakota border. Approximately 10,000 acres of crops were completely destroyed, and combined monetary damages to crops and property approached 35 million USD. Although supercell storms are not particularly common in Montana, the sheer duration and severity of this event distinguish it from other organized severe convective episodes. This paper documents the pre-storm environment and evolution of this supercell within an atmosphere characterized by very limited instability, yet pronounced shear.

Synoptic and Mesoscale Environment

At 1200 UTC 16 June 2007, an upper low embedded within a mobile upper tropospheric trough was situated near Vancouver Island resulting in southwest upper flow across the Northern Rocky Mountains (Figure 1). From a climatological standpoint, the majority of organized severe convective episodes in the Northwestern United States occur within this flow regime (Evenson and Johns 1995). At 300 hPa, a 100 knot cyclonically-curved jet streak was present across northern Oregon with a 90 knot anticyclonic jet streak extending from lower Alberta into Saskatchewan. Thermal ridging was apparent at 700 hPa across western Montana with thermal packing extending into South Dakota along a marked frontal boundary. This boundary was also apparent at 850 hPa and both the morning surface and satellite analyses revealed a stationary front draped along the lee of the Montana Rockies. North of this boundary, surface high pressure in lower Saskatchewan maintained relatively cool, yet moist low level easterly trajectories throughout eastern Montana (Figure 2). Surface dewpoints within this flow averaged around 10° C. In anticipation of potentially significant severe convection, the Storm Prediction Center categorized much of central and southeast Montana within a moderate risk for severe thunderstorms (Figure 3).

Morning and afternoon visible satellite imagery indicated a persistent band of mid-level clouds lifting northward across eastern Montana. Gridded model data from the GFS, NAM-WRF and RUC indicated this cloud band was driven by increasingly positive 850 hPa to 500 hPa warm air advection in response to divergence within the right entrance region of the anticyclonic upper jet streak. Consequently, 2-D frontogenesis fields across northeast Montana underwent pronounced intensification (Figure 4). Special 1800 UTC upper air soundings were launched from both Great Falls and Glasgow; hereafter TFX and GGW, respectively. The profile from the GGW sounding revealed a southeasterly flow around 15 knots extending from the surface up to

approximately 2 km AGL with predominantly pseudo-moist adiabatic lapse rates above 1 km AGL (Figure 5). Surface Based CAPE (SBCAPE) was practically non-existent due to substantial convective inhibition; however 220 J/kg of elevated CAPE did exist above a moist mid level inversion near 570 hPa. By early afternoon this elevated instability manifested itself in the form of well developed ACCAS over GGW thereby confirming the aforementioned jet differential vorticity advection. Although the surface frontal boundary never advanced to within 129 km (80 miles) of GGW this day, continued deepening of the mixed layer throughout the afternoon north of the boundary did result in marginal SBCAPE across northeast Montana. Early afternoon 0-6 km bulk shear values of 60 knots at TFX and 50 knots at GGW were already within the favored shear threshold for supercells.

The 0000 UTC 17 June 2007 GGW sounding terminated short of the equilibrium level (EL), so upon applying the EL from the afternoon sounding SBCAPE was found to have increased to 774 J/kg (Figure 6). However, the richest low level moisture was quite shallow (roughly 500 feet) and a Mean Layer CAPE (MLCAPE) calculation resulted in just 581 J/kg. MLCAPE has been shown to be more representative of available instability especially in environments characterized by shallow low level moisture or when the primary forcing is rooted above the boundary layer (Thompson et al. 2003). A comparison of these MLCAPE values with GOES sounder derived CAPE indices revealed reasonable consistency.

Despite the limited instability, shear had increased markedly from the afternoon sounding. Pronounced low level turning evident on the 0000 UTC June 17 GGW hodograph resulted in 0-3 km SRH values of $369 \text{ m}^2/\text{s}^2$ while 0-6 km bulk shear climbed to 78 knots. LAPS data from 0000 UTC indicated 0-3 km environmental helicity values of nearly $800 \text{ m}^2/\text{s}^2$ embedded within SBCAPE of just 700 J/kg (Figure 7). Despite the deceptively low instability, environments characterized by marginal CAPE and strong shear can support organized convection, including supercells, so long as sufficient updraft rotation develops. The dynamically induced pressure gradient force within the mesocyclone compensates for limited instability thereby resulting in greater updraft velocities than would be found with a non-rotating storm in the same environment (Weisman and Klemp, 1984).

The GGW evening sounding (Figure 6) also showed a lowering of the moist mid-level inversion previously at 600 hPa to 700 hPa coincident with sharply veered winds from 600-700 hPa indicating even stronger isentropic ascent. Strong afternoon low level mixing had deepened the boundary layer to 3 km (9842 ft) AGL and, when combined with limited low level moisture, a pronounced inverted V structure developed. Compared to the afternoon sounding, the 0000 UTC WBZ height had increased from 2.3 km (7538 ft) AGL to 2.9 km (9520 ft) AGL, although this was still at a preferred level for hail production. In addition, sufficient CAPE in the -10° C to -30° C layer would enhance hail growth while at the same time hail melt would be suppressed given a dry sub cloud layer with LCL heights of 1.7 km (5577ft) AGL. The presence of this relatively dry and well mixed boundary layer also supported nearly 1000 J/kg of downdraft CAPE thereby enhancing convective gusts.

Supercell Evolution

Favored coupling of two 300 hPa jet streaks supported persistent upper level ageostrophic divergence across northwest Montana by late morning (Figure 8). Earlier in the morning, visible satellite imagery revealed the presence of enhanced convective growth within the exit region of the western-most jet streak (Figure 2), and by 1654 UTC this convection had impinged on the area of enhanced upper divergence resulting in a rapid escalation of convective activity. The most organized thunderstorm cell within this activity initiated approximately 120 km north of TFX, or about 385 km west-northwest of GGW, in Toole County, Montana. Over the course of the next 44 minutes, the TFX WSR-88D measured an initial reflectivity core of 50 dbZ at 13,000 ft AGL having increased to 55 dbZ at 23,000 ft AGL. It was during this intensification that the storm began turning right of its initial northeast motion while displaying a mesocyclone in the mid levels coincident with a weak echo region (WER) up to 18,000 ft AGL. The -20° C level, as measured by the 1800 UTC TFX sounding, was shown to be 18,000 ft AGL and with greater than 50 dbZ above this, there exists reasonable confidence that severe hail growth was already in progress. The first severe weather report received was of 1.9 cm (0.75 inch) hail at 1840 UTC near Gildford, MT. For the next three hours this supercell storm maintained an easterly motion into Blaine County; although radar data was soon restricted to the mid and upper portions of the storm given the storm's substantial displacement from both the TFX and GGW radars.

Through 2100 UTC June 16 the supercell underwent additional strengthening as the reflectivity core increased to 65 dbZ at 9 km (30,000 ft) AGL while the storm motion deviated to the southeast. The Storm Prediction Center had issued a tornado watch for much of central Montana at 2020 UTC and at 2125 UTC a tornado warning was issued for northern Phillips county after trained storm spotters observed a funnel cloud northwest of Dodson. As this supercell proceeded through Phillips County, the lowest radar tilt from GGW provided more information concerning the storm's low level structure. A strong low level inflow notch and hook echo became apparent at 2203 UTC (Figure 10) and storm relative velocity data revealed the mesocyclone had descended to 1.5 km (5032 ft) AGL with 120 knots of gate to gate shear. Also at this time a well developed BWER structure extended from the mesocyclone south nearly 6.4 km (21,000 ft) in length up to a maximum height of 6.7 km (22,000 ft) AGL. By 2241 UTC, a mid-altitude radial convergence signature approximately 10 km (33,000 ft) in length developed at a height of 4.9 km (16,000 ft) AGL and was followed by a strengthening Rear Inflow Notch (RIN) within the lowest tilts of reflectivity. Wind velocities within the RIN averaged 55 knots and by 2310 UTC a bow echo structure culminated just south of the supercell's mesocyclone.

Throughout the bow echo development, the BWER doubled in length to nearly 13 km (42,650 ft) while having maintained a peak depth of 7 km (22,965 ft) AGL. The significance of this expanding BWER was identified and termed a "Deep Convergence Zone (DCZ)" by Lemon and Burgess in 1992 and accounted for the unusual longevity and prominence of elongated BWERs within some supercells; especially those associated with prolific hailstorms (Figure 9). Consistent with findings from a study by Lemon and Parker in 1996, both spectrum width and velocity data from the KGGW radar revealed narrow, yet intense gradients of turbulent mixing and shear just ahead of the supercell's reflectivity core extending up the majority of the storm's depth.

In order for the DCZ structure to persist, a steady balance between storm outflow and inflow must exist (Lemon and Parker, 1996). The inflow portion of this balance became apparent at 2338 UTC when the GGW ASOS measured a 54 knot (62 miles/hr) inflow gust directly out of the east into the updraft located 8 km (5 miles) west of the ASOS. Just over 30 minutes later, an outflow gust of 77 knots (89 miles/hr) was measured by a weather spotter 11 km (7 miles) south of GGW near the apex of the bow echo. Due to the low density of surface observations across northeast Montana, it is plausible that the inflow velocities with this supercell exceeded that measured by the ASOS in GGW.

GGW radar indicated the mesocyclone became displaced to the northwest of the bow echo at 2340 UTC as rotational velocities in the lowest levels underwent gradual diminishment. Despite the weaker velocity couplet, a trained weather spotter reported a funnel cloud minutes earlier near Tampico justifying the issuance of another tornado warning. At 2354 UTC large hail up to baseball size commenced at GGW followed by much smaller hail with flooding rains over the course of the next 23 minutes. Property damage in GGW was widespread and consisted primarily of broken windows, damaged roofing and siding, and numerous downed tree limbs.

Over the course of the next three hours this high precipitation supercell maintained a deviant southeast storm motion across McCone and Richland Counties with numerous reports of wind-driven hail. Interestingly, the length of the DCZ diminished considerably from 13 km (42,650 ft) to just 4.5 km (14,784 ft) by 0142 UTC. LAPS data from 0200 UTC across eastern Montana displayed an environment more hostile for supercells as MLCAPE fell to 300 J/kg while more importantly 0-3 km SRH values decreased to just 50 m²/s². Consequently, subsequent GGW radar returns revealed a marked decay in both the supercell's mesocyclonic rotation and maximum reflectivity core height as the storm approached Sidney, MT (Figure 11). Interrogation of the storm's lowest levels and any means of identifying circulations within were no longer possible given nearly 160 km (100 miles) separation from the GGW radar; however, considering the aforementioned trends and an observed shift in storm motion from southeast to east-northeast, it was apparent that supercellular traits had ceased by 0328 UTC.

Despite one initial report of a funnel cloud and pronounced low level rotational velocities at various times, ground and aerial surveys in addition to follow-up interviews with storm spotters revealed no evidence of any tornado. Interestingly, throughout much of the event the pre-storm environment was characterized by appreciable 0-1 km shear of up to 30 knots. This value is well within favored thresholds established for supercellular tornadoes, especially those deemed significant by Craven et al. (2004). Ignoring modification of the near storm environment, a consideration of additional tornado forecast parameters indicated relatively high MLLCL heights of 1.8 km (6000 ft) AGL and limited 0-3 km CAPE values of only 20 J/kg. These values supported a lower probability for tornadoes even with considerable 0-1 km shear present.

In the days following the event, sufficient clearing of clouds permitted the viewing of an impressive hailswath from visible satellite (Figure 12). The occurrence of record rainfalls in May across northeast Montana supported lush vegetation thereby allowing widespread crop damage. Measurements indicated this hailswath was approximately 459 km (285 miles) long and up to 16 km (10 miles) wide at times.

Conclusion

Although rare, events such as this underscore the need for the forecaster to maintain situational awareness when confronted with patterns exhibiting deceptively small CAPE embedded within strong shear and background forcing. As was the case in this event, the presence of sustained isentropic ascent provided sufficient forcing to maintain an isolated thunderstorm, and through mesocyclonic pressure deficits, overcome the limited buoyancy and persisted for an exceptionally long time. Unfortunately, the ability to successfully anticipate the development of a convective storm of this magnitude and duration remains a challenge given limitations within high resolution gridded models, especially with regard to these models accurately forecasting convective behaviors. However, pattern recognition combined with routine analysis of observed data can greatly assist the forecaster in discriminating the probability of occurrence for similar events.

References

- Craven, Jeffrey P., and Harold E. Brooks, 2004: Baseline Climatology of Sounding Derived Parameters Associated with Deep Moist Convection. *National Weather Digest*, 28, 13-24.
- Davies, J., M., 2002: On Low-Level Thermodynamic Parameters Associated with Tornadic and Non-Tornadic Supercells. Preprints, 21st Conf. on Severe Local Storms, San Antonio, TX, Amer. Meteor. Soc., P12.5.
- Evenson, E.C., and R.H. Johns, 1995: Some Climatological and Synoptic Aspects of Severe Weather Development in the Northwestern United States. *National Weather Digest*, 20, 1, 34-50.
- Lemon, L.R. and S. Parker, 1996: The Lahoma Storm Deep Convergence Zone: Its Characteristics and Role in Storm Dynamics and Severity. Preprints, 18th Conf. Severe Local Storms, San Francisco, Amer. Meteor. Soc., 70-75.
- Markowski, P., C. Hannon, J. Frame, E. Lancaster, A. Pietrycha, R. Edwards, and R.L. Thompson, 2003: Characteristics of Vertical Wind Profiles near Supercells Obtained from the Rapid Update Cycle. *Wea. Forecasting*, 18, 1262–1272.
- Thompson, R. L., R. Edwards, J. A. Hart, K. L. Elmore, and P. Markowski, 2003: Close Proximity Soundings within Supercell Environments Obtained from the Rapid Update Cycle. *Wea. Forecasting*, 18, 1243-1261.
- Weisman, M.L., and J.B. Klemp, 1984: The Structure and Classification of Numerically Simulated Convective Storms in Directionally Varying Wind Shears. *Mon. Wea. Rev.*, 112, 2479–2498.

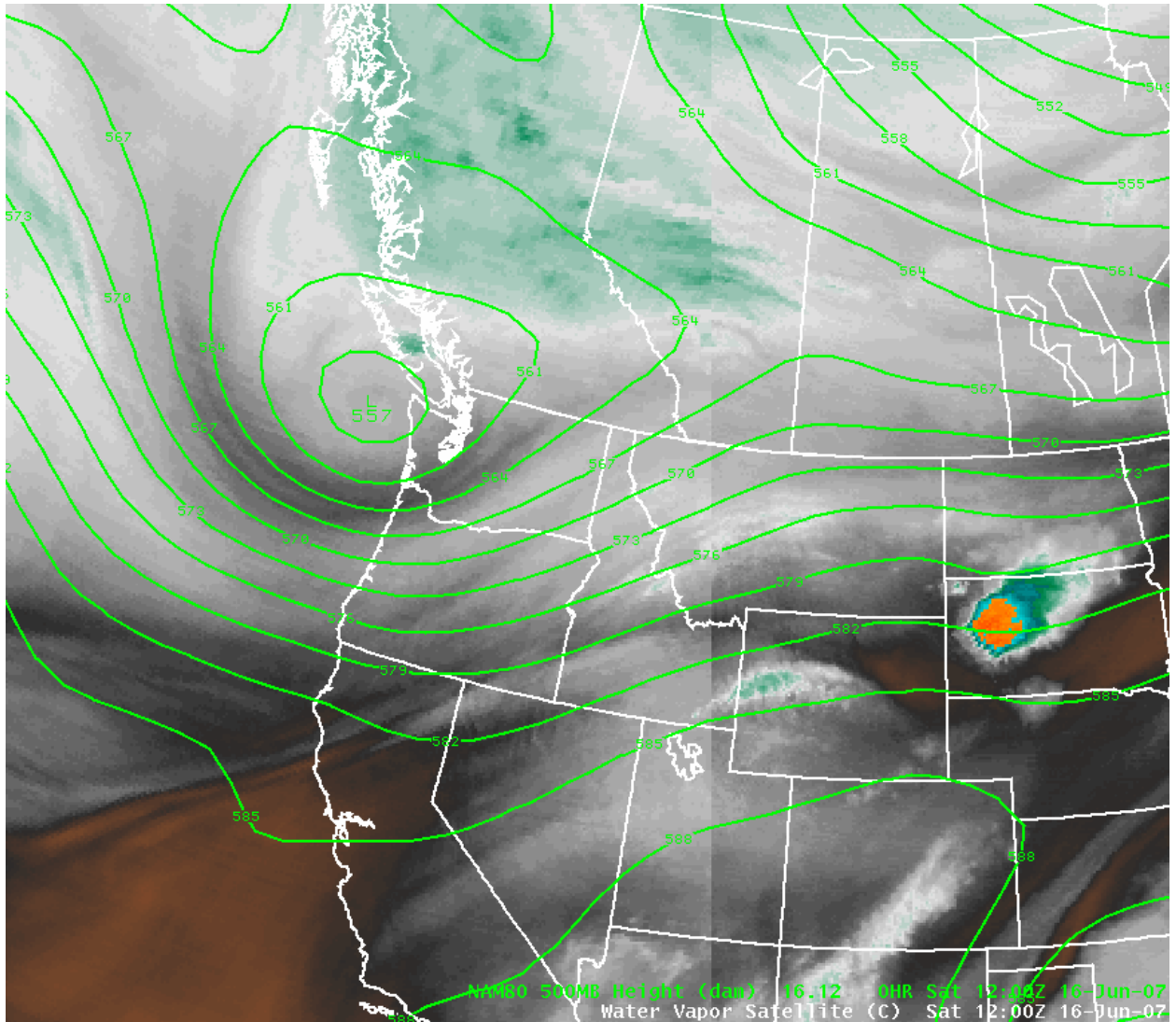


Figure 1: 1200 UTC 16 June 2007 water vapor image with NAM-WRF 500 hPa heights overlaid.

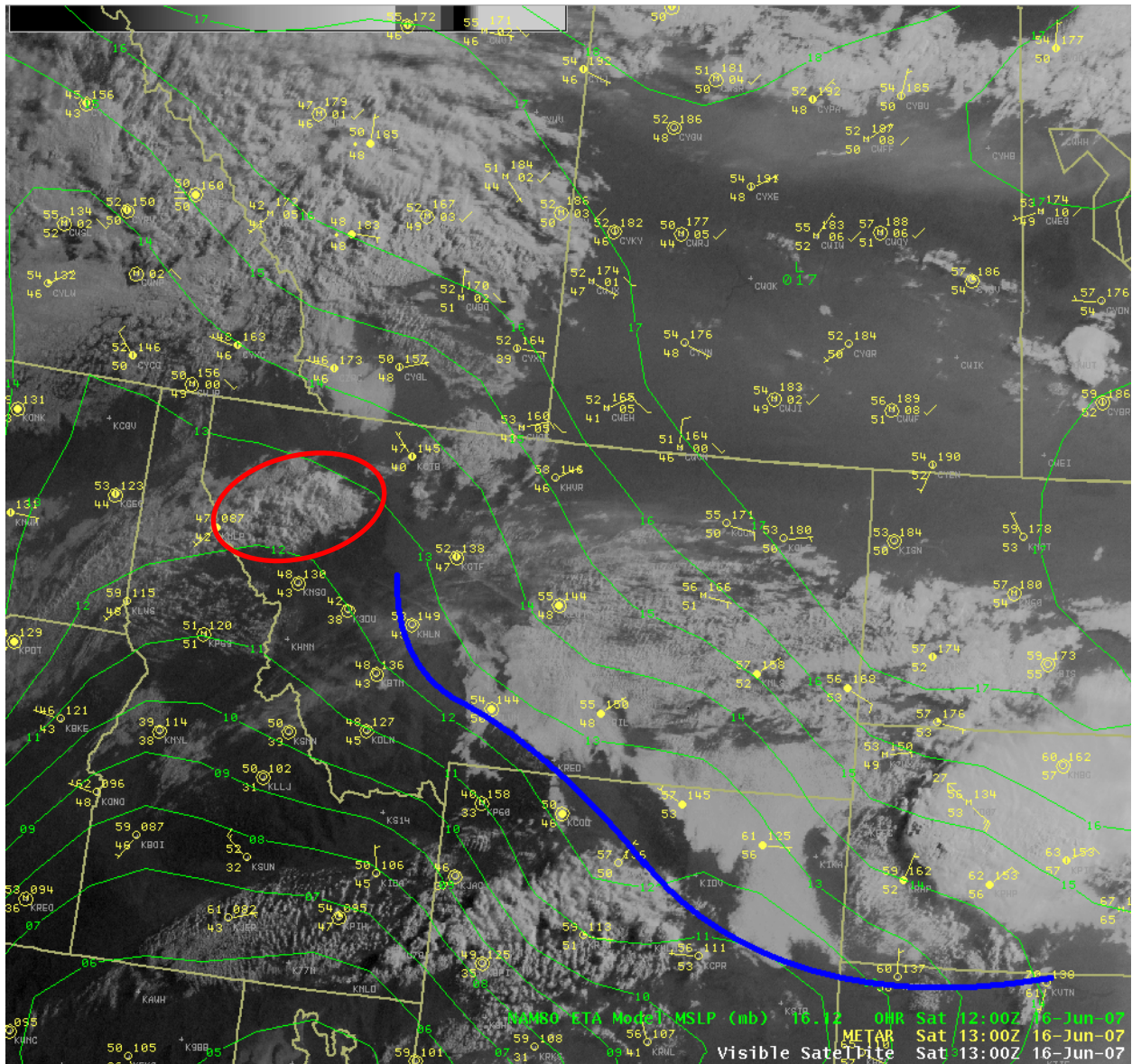


Figure 2: 1300 UTC June 16 surface observations and visible satellite, 12 UTC NAM-WRF MSLP, and surface frontal boundary in blue. An area of enhanced convection (enclosed by the circle) would later evolve into the long-lived supercell. Temperature and dewpoint are plotted in degrees Fahrenheit.

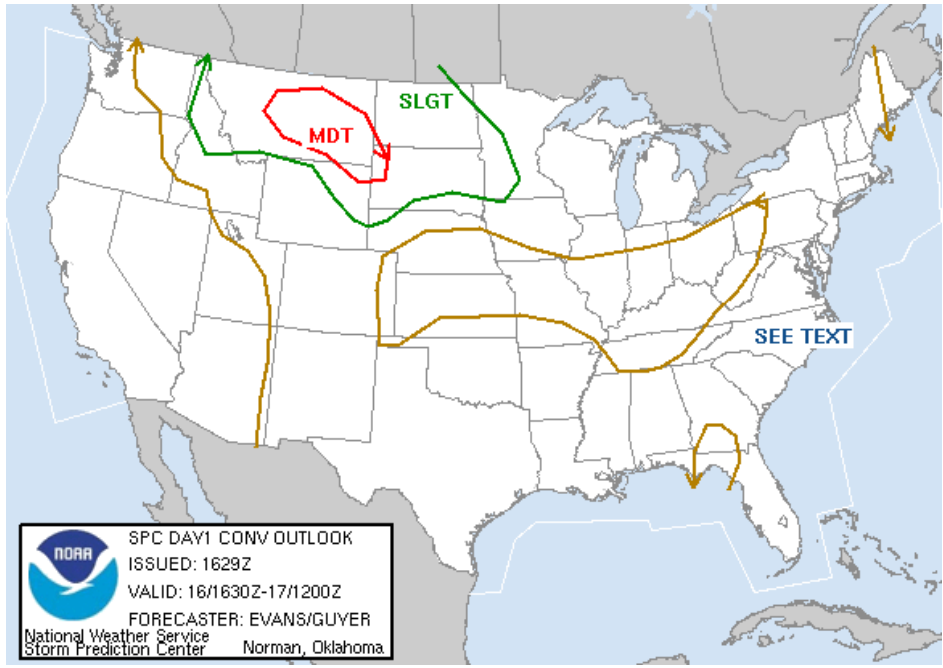


Figure 3: 1630 UTC day one convective outlook from the Storm Prediction Center.

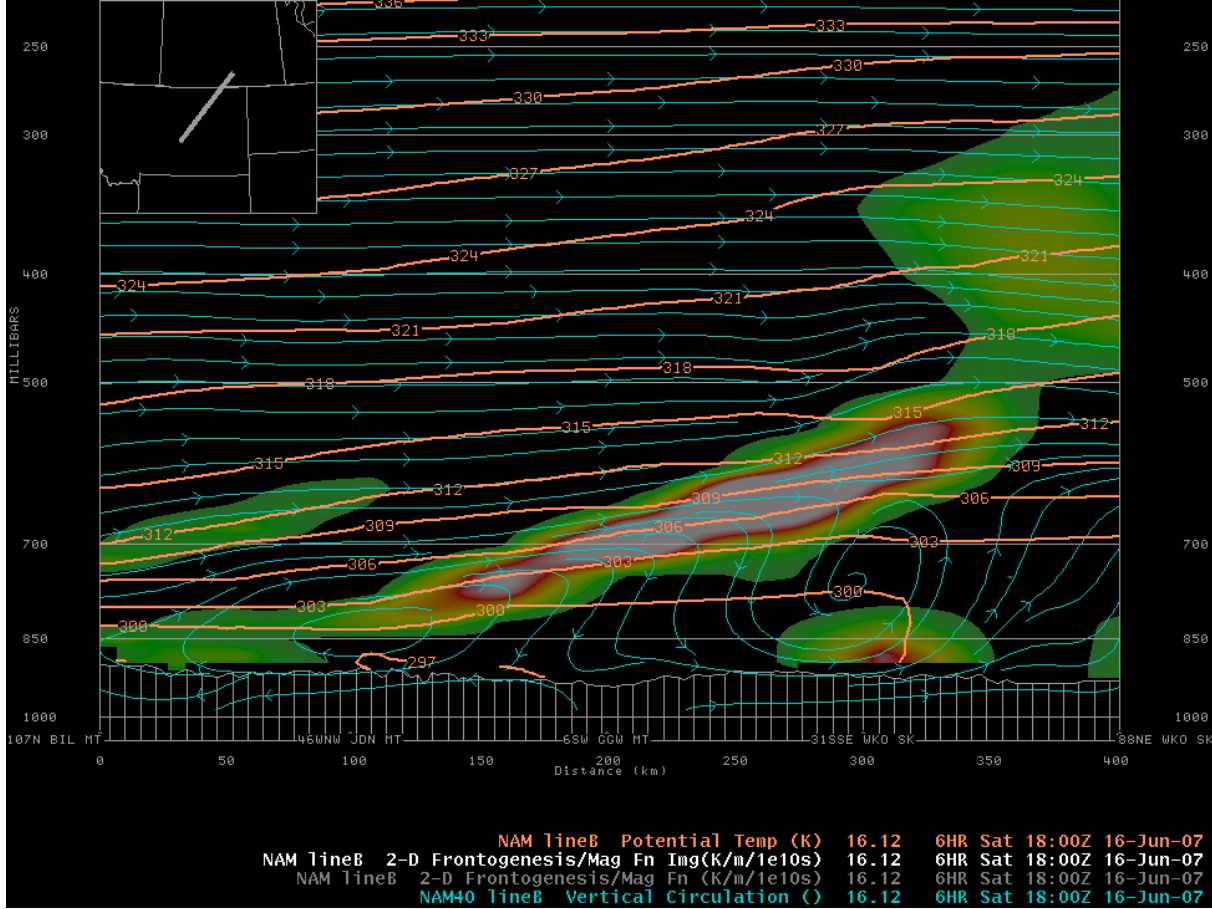


Figure 4: 1800 UTC NAM-WRF cross section of potential temperature, 2-D frontogenesis and the vertical circulation component across northeast Montana.

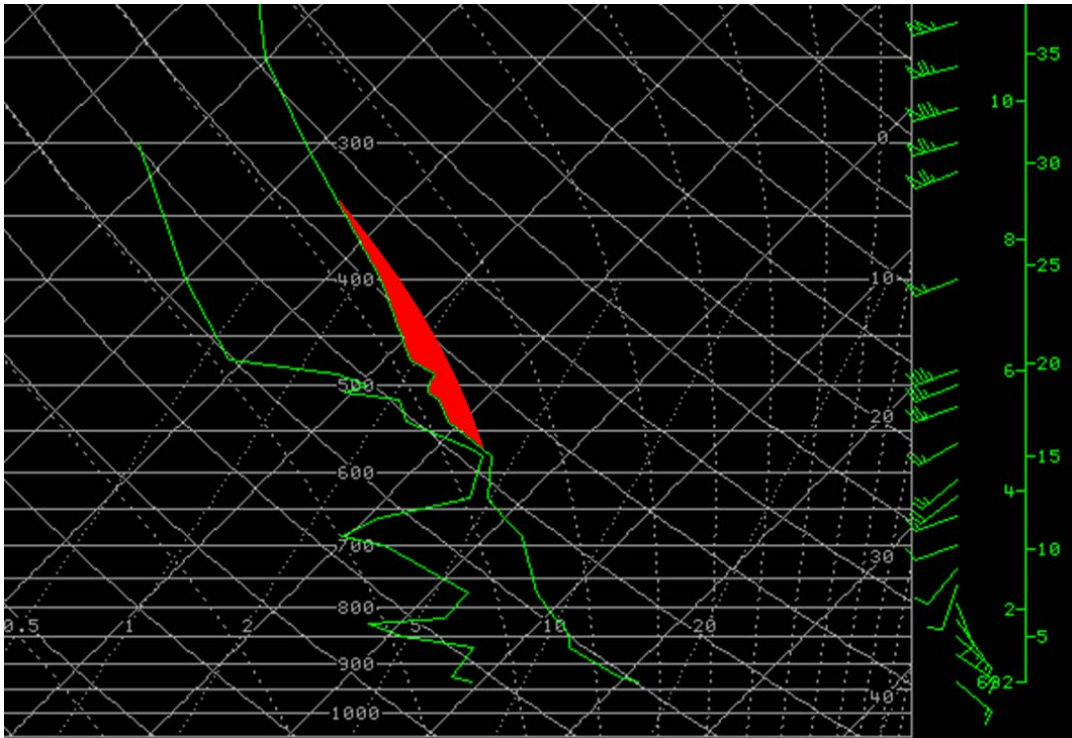


Figure 5: 16 June 1800 UTC GGW observed sounding revealing sufficient shear with a shallow layer of elevated CAPE highlighted in red.

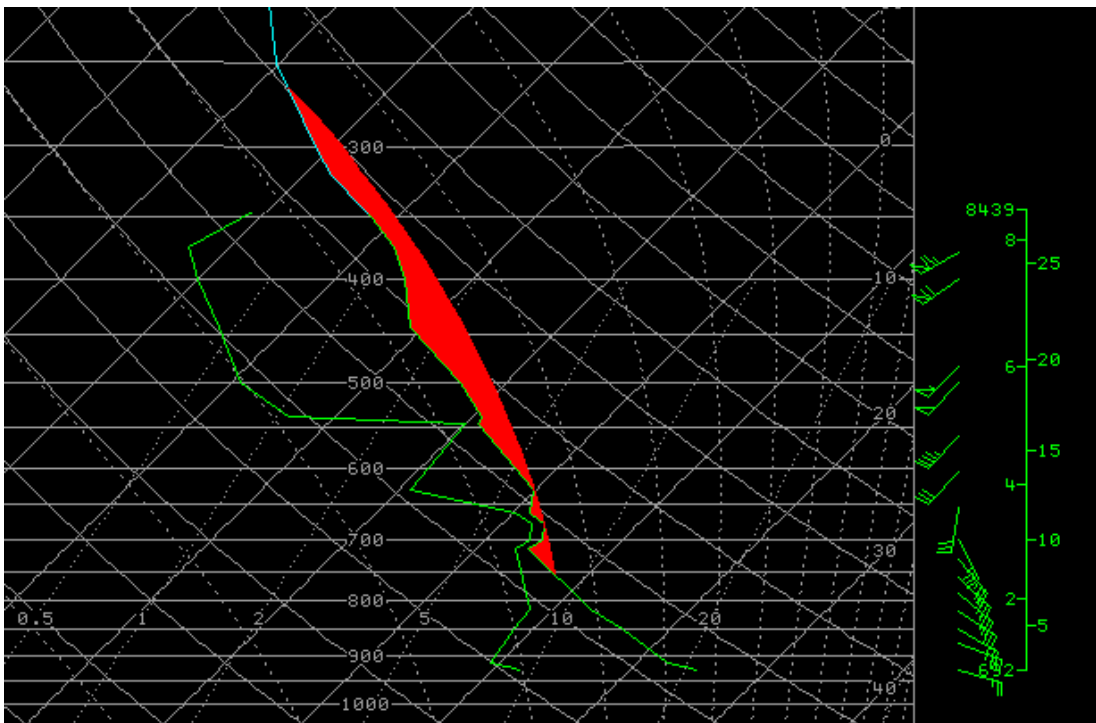


Figure 6: 0000 UTC June 17 GGW observed sounding up to 350 hPa with data above this level acquired from the 1800 UTC June 16 GGW sounding. The shaded profile represents MLCAPE using an average of the lowest 100 hPa for the lifted parcel. Note the marked increase in shear throughout the profile contrasted with that shown in Figure 5.

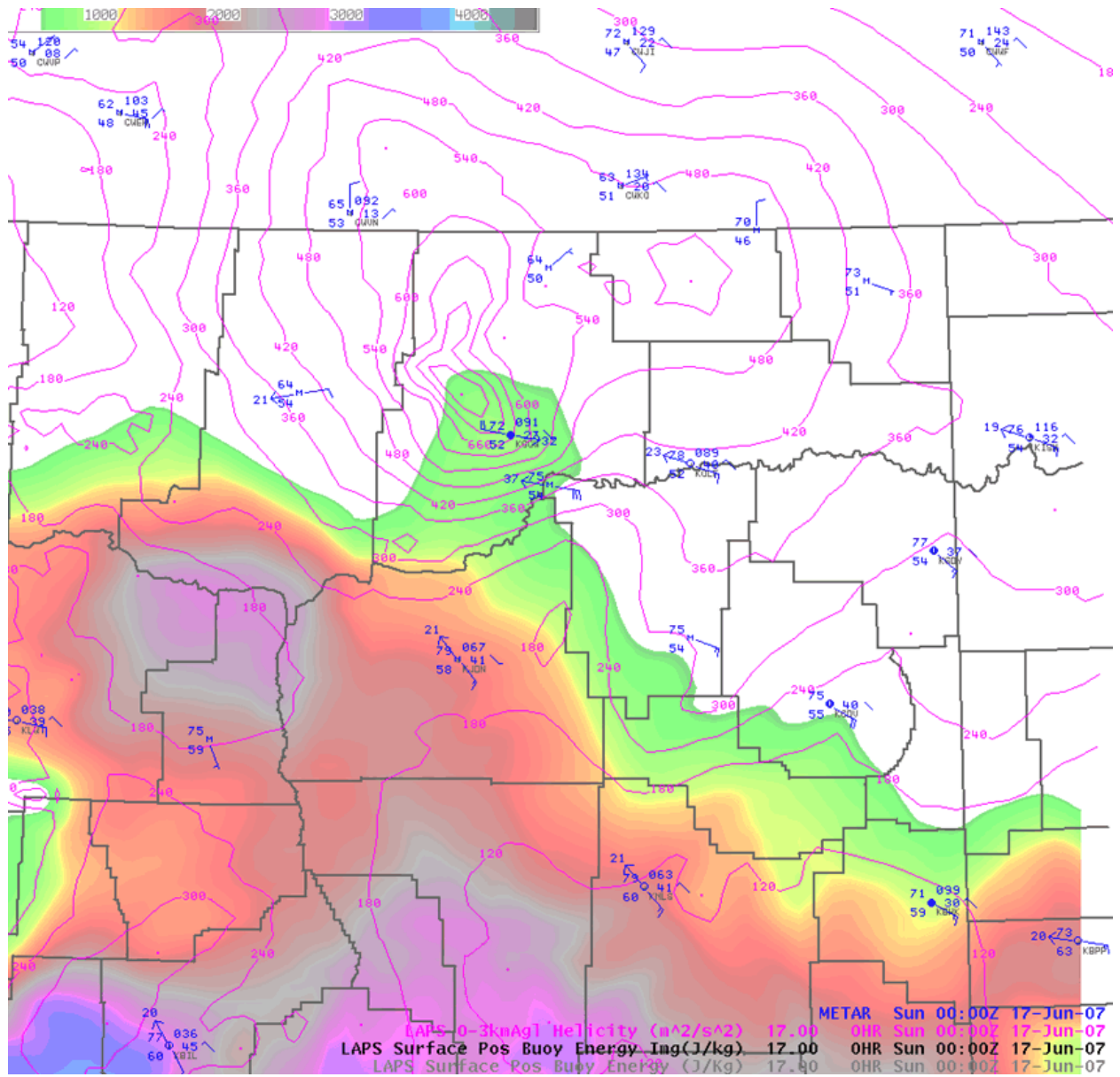


Figure 7: Surface observations across northeast Montana at 00 UTC June 17 overlaid with LAPS SBCAPE (loaded as image) and 0-3 km helicity isopleths in 60 m²/s² intervals.

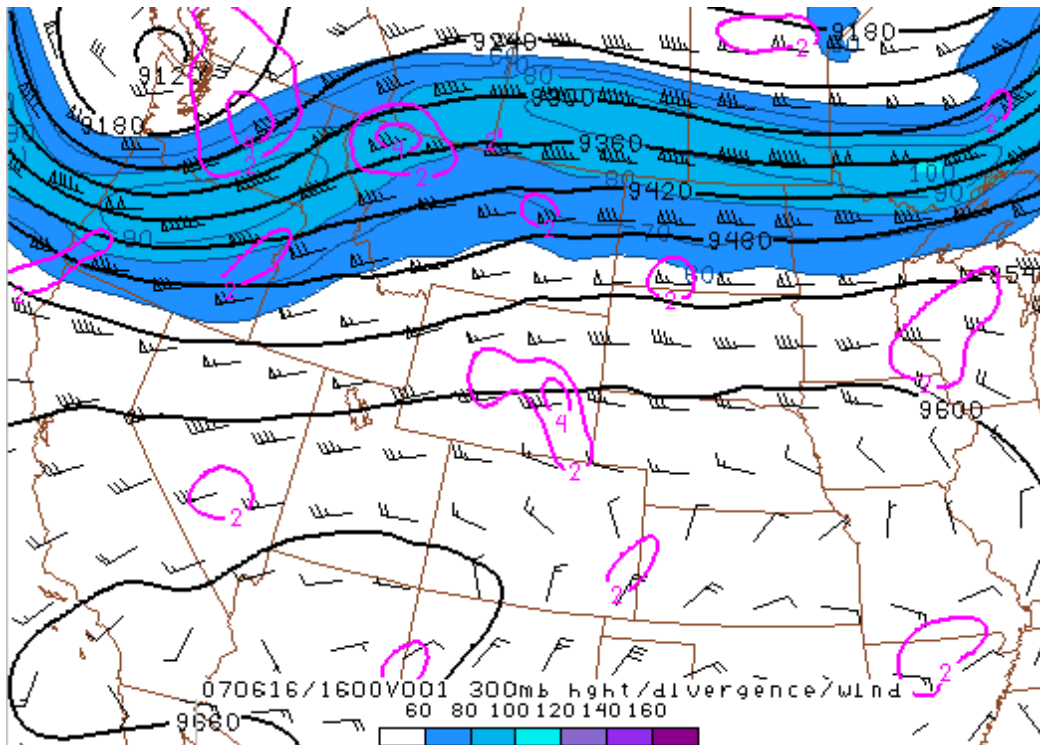


Figure 8: 1600 UTC RUC 300 hPa heights, winds, isotachs (shaded ≥ 60 knots at 10 knot intervals), and divergence. An area of persistent divergence resides in northwest Montana given favorable coupling between the cyclonic jet streak upstream and an anticyclonic jet streak just downstream.

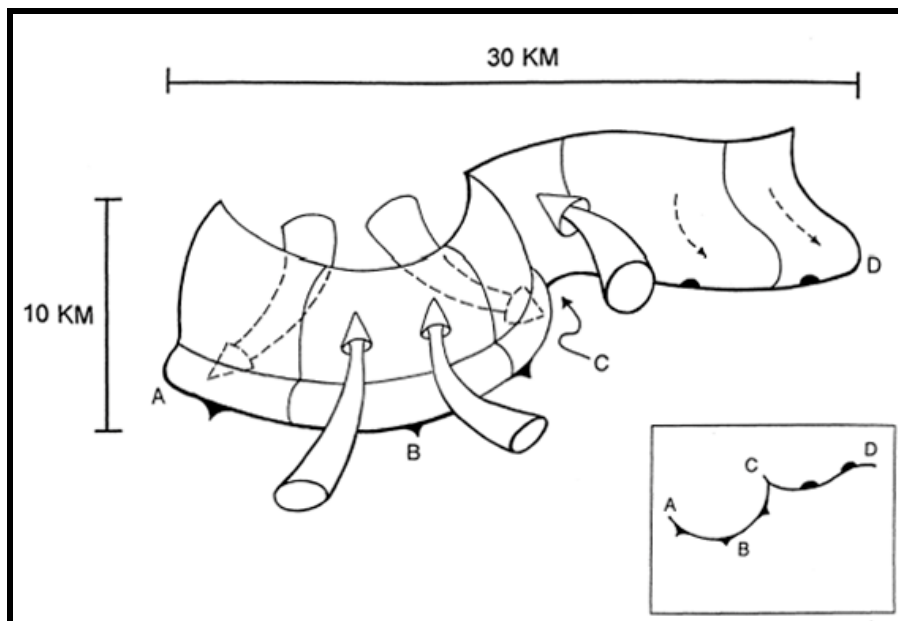


Figure 9: Three-dimensional, synthesized, Deep Convergence Zone schematic through supercell mesocyclone. Inset is plan view. Supercell updraft is located from B to C with BWER, and storm summit in the vicinity of B. Arrows indicate storm-relative flow; dashed arrows indicate, in perspective, flow behind the DCZ surface. Storm motion is toward reader. Schematic and description from Lemon and Parker, 1996.

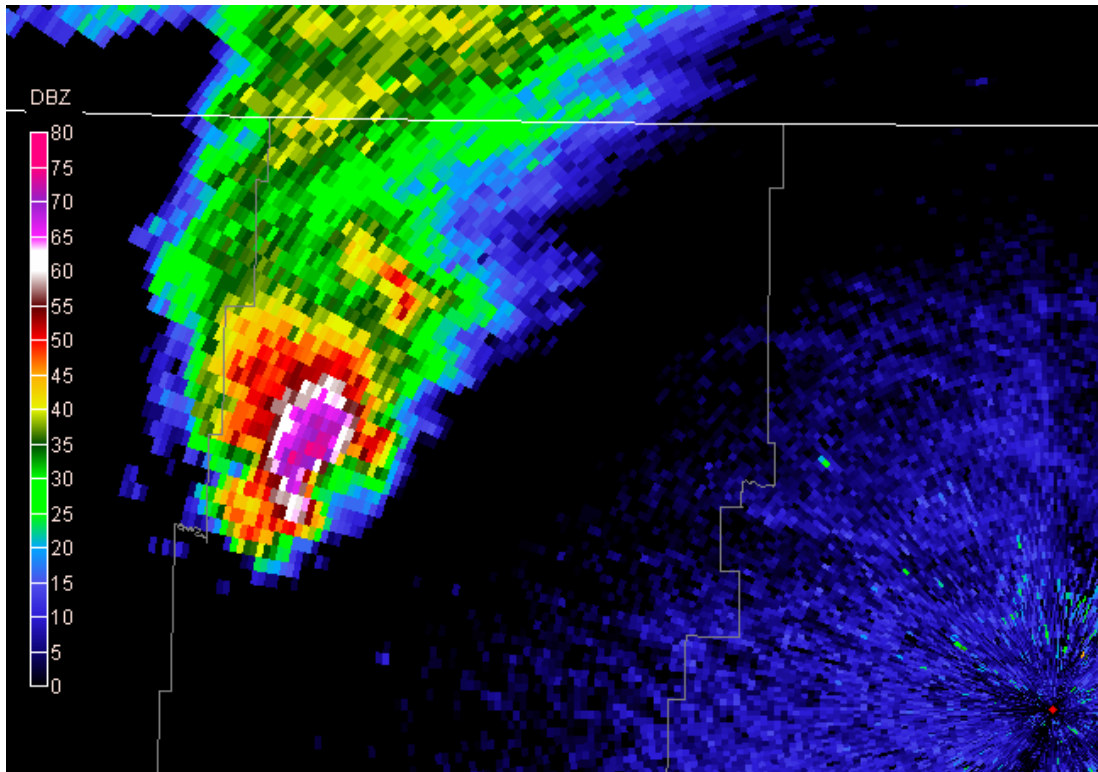


Figure 10: 2203 UTC GGW 0.5 degree reflectivity image depicting a low level inflow notch and hook echo. The GGW radar is located at the bottom right.

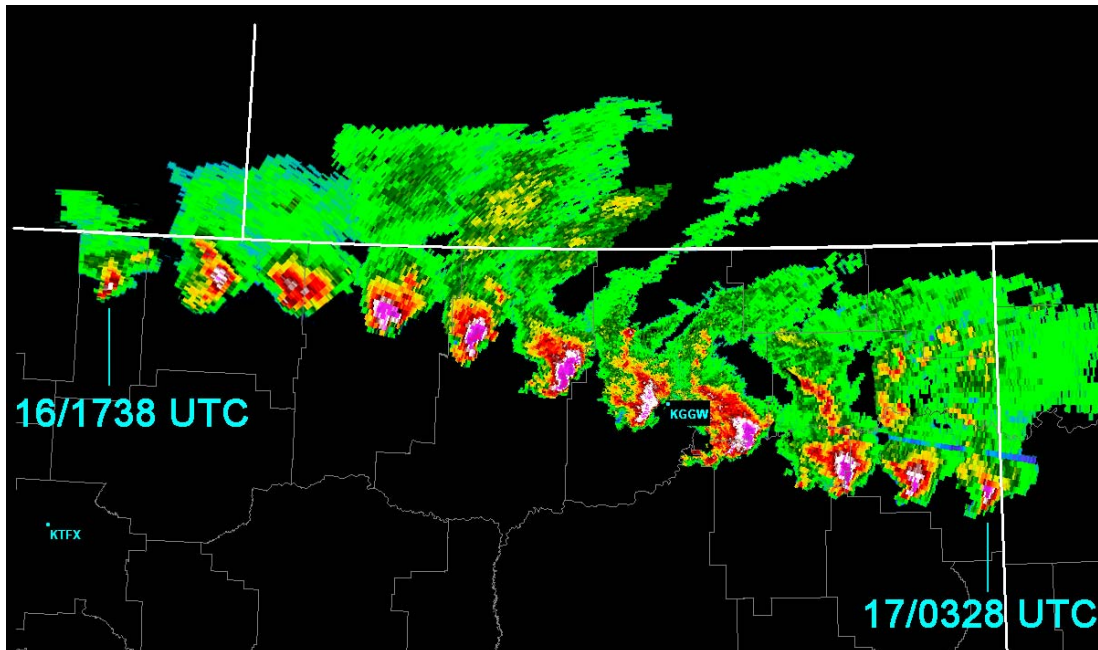


Figure 11: Combined TFX and GGW 0.5 degree reflectivity tilts beginning at 1738 UTC June 16 and ending at 0328 UTC June 17. The radar data step interval is approximately 60 minutes.

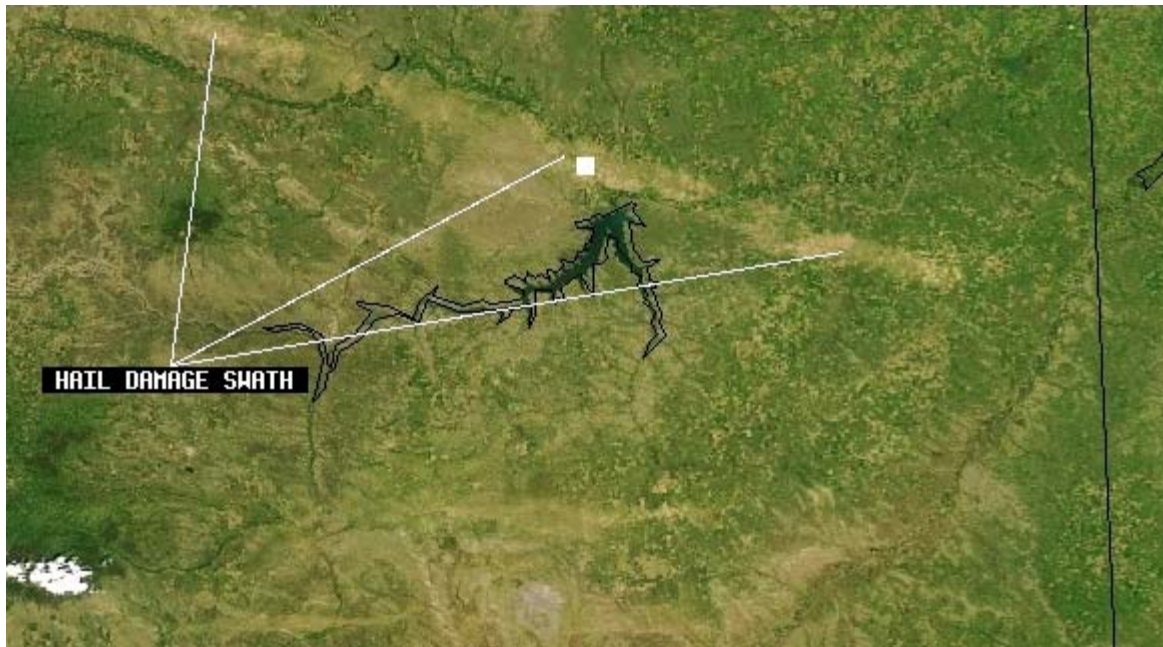


Figure 12: Eastern extent of a significant hailswath visible from the Aqua MODIS satellite. The square corresponds to Glasgow, MT.